

Numerical Analysis of the Helmholtz Green's Function for Scalar Wave Propagation Through a Nano-hole on a Plasmonic Layer

Désiré Miessein,^{1,2} Norman J. M. Horing,² Godfrey Gumbs,^{3,4} and Harry Lenzing²

¹*Department of Physics and Engineering Physics,
Fordham University, Bronx, New York 10458, USA*

²*Department of Physics and Engineering Physics,
Stevens Institute of Technology, Hoboken, New Jersey 07030, USA*

³*Department of Physics and Astronomy,
Hunter College of the City University of New York, New York, NY 10065, USA*

⁴*Donostia International Physics Center (DIPC),
P de Manuel Lardizabal, 4, 20018 San Sebastian, Basque Country, Spain*

(Dated: December 1, 2021)

Abstract

A detailed numerical study of the Helmholtz Green's function for the description of scalar wave propagation through a nano-hole on a plasmonic layer is presented here. In conjunction with this, we briefly review the analytic formulation taking the nano-hole radius as the smallest length parameter of the system. Figures exhibiting the numerical results for this Green's function in various ranges of the transmission region are presented.

PACS numbers:

1. INTRODUCTION

The transmission properties of a scalar field propagating through a nano-hole in a two-dimensional (2D) plasmonic layer have been analyzed using a Green's function technique in conjunction with an integral equation formulation [1,2,3,4]. The nano-hole is taken to lie on a plasmonic sheet (located on the plane $z = 0$ embedded in a three-dimensional (3D) bulk host medium with background dielectric constant $\varepsilon_b^{(3D)}$). In Section II of this paper, we briefly review in some detail the analytic determination of the scalar Helmholtz Green's function

with the presence of the layer in which a two-dimensional plasma is embedded. Section III reviews the scalar Helmholtz Green's function solution for the 2D plasmonic layer embedded in a 3D host medium with the presence of a nano-hole aperture in the subwavelength regime. The results of our thorough numerical analysis of the perforated layer Helmholtz Green's function are discussed in Section IV with illustrative figures showing results in the near, middle and far field zones of the transmission region. Finally, conclusions are summarized in Section V.

2. GREEN'S FUNCTION SOLUTION FOR FULL 2D PLASMONIC LAYER EMBEDDED IN A 3D BULK HOST MEDIUM

2.1. Integral Equation for the Scalar Green's Function and Solution

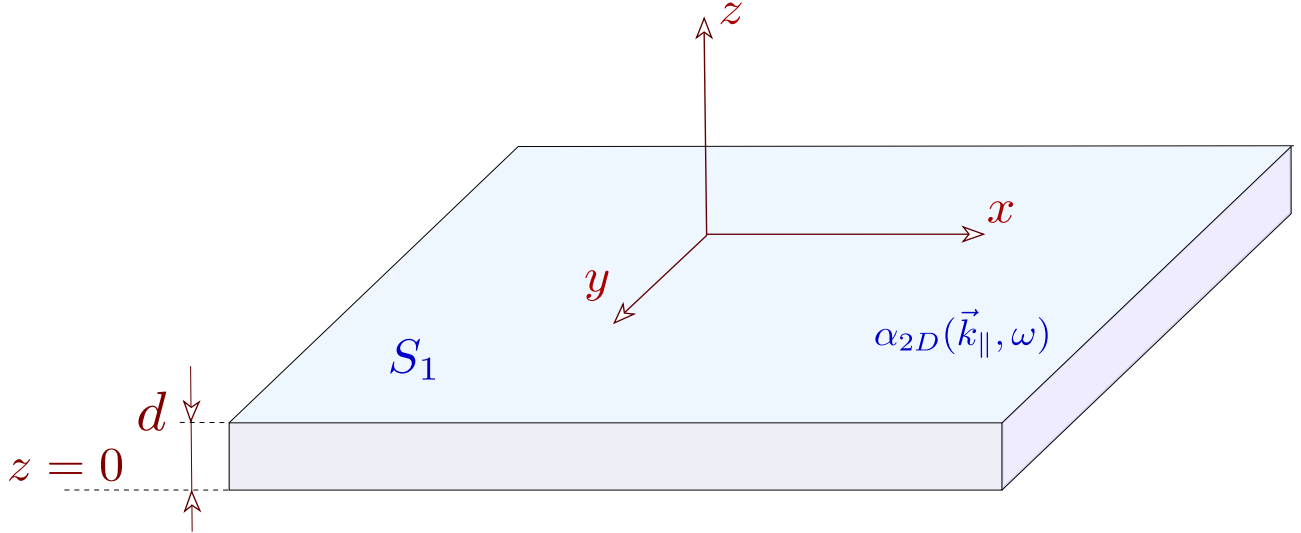


FIG. 2.1.1: (Color online) Schematic illustration of a two dimensional plasmonic layer S_1 of thickness d embedded at $z = 0$ in a three dimensional bulk medium with dielectric constant $\varepsilon_b^{(3D)}$.

We consider a two dimensional plasmonic layer S_1 to have a dynamic nonlocal 2D polarizability $\alpha^{(2D)}(\vec{k}_{||}, \omega)$, located on the plane $z = 0$, embedded in a three dimensional bulk host medium with background dielectric constant $\varepsilon_b^{(3D)}$ (Fig.2.1.1). The associated Helmholtz Green's function including the two-dimensional plasmonic sheet, G_{fs} *without* a nano-hole, satisfies the integro-differential equation (position/frequency representation)[1,2,3,4]

$$\left(-\vec{\nabla}^2 - \frac{\omega^2}{c^2}\varepsilon_b^{(3D)}\right) G_{fs}(\vec{r}, \vec{r}'; \omega) - \frac{\omega^2}{c^2} \int d^3\vec{r}'' \alpha_{fs}^{(2D)}(\vec{r}, \vec{r}''; \omega) G_{fs}(\vec{r}'', \vec{r}'; \omega) = \delta^{(3)}(\vec{r} - \vec{r}'). \quad (2.1.1)$$

The polarizability $\alpha_{fs}^{(2D)}$ of the full 2D plasmonic layer has the form

$$\alpha_{fs}^{(2D)}(\vec{r}, \vec{r}'; \omega) = \alpha_{fs}^{(2D)}(\vec{r}_{||}, \vec{r}'_{||}; \omega) d \delta(z) \delta(z') \quad (2.1.2)$$

where d is the thickness of the plasmonic sheet, $\vec{r} = (\vec{r}_{||}; z)$ and $\alpha_{fs}^{(2D)}(\vec{r}_{||}, \vec{r}'_{||}; \omega)$ is the 2D plasmonic polarizability of the 2D sheet; $\delta(z)$ is the Dirac delta function needed to confine the polarizability onto the plane of the 2D layer at $z = 0$.

To solve Eq. (2.1.1), we employ the bulk Helmholtz Green's function [5]

$$\left(-\vec{\nabla}^2 - \frac{\omega^2}{c^2}\varepsilon_b^{(3D)}\right) G_{3D}(\vec{r}, \vec{r}'; \omega) = \delta^{3D}(\vec{r} - \vec{r}'). \quad (2.1.3)$$

After performing the 2D spatial Fourier transform of G_{3D} in the plane of the translationally invariant 2D homogeneous plasmonic sheet ($\vec{r}_{\parallel} = \vec{r}_{\parallel} - \vec{r}'_{\parallel}$)

$$G_{3D}(\vec{k}_{\parallel}; z, z'; \omega) = \int d^2\vec{r}_{\parallel} G_{3D}(\vec{r}_{\parallel}; z, z'; \omega) e^{-i\vec{k}_{\parallel}\cdot\vec{r}_{\parallel}}, \quad (2.1.4)$$

equation (2.1.3) becomes

$$\left[\frac{\partial^2}{\partial z^2} + k_{\perp}^2\right] G_{3D}(\vec{k}_{\parallel}; z, z'; \omega) = -\delta(z - z') \quad (2.1.5)$$

where $k_{\perp}^2 = q_{\omega}^2 - k_{\parallel}^2$ and $q_{\omega} = \frac{\omega}{c}\sqrt{\varepsilon_b^{(3D)}}$. This has the well-known solution [5]

$$G_{3D}(\vec{k}_{\parallel}; z, z'; \omega) = -\frac{e^{ik_{\perp}|z-z'|}}{2ik_{\perp}}. \quad (2.1.6)$$

Employing $G_{3D}(\vec{r}, \vec{r}'; \omega)$, Eq. (2.1.1) can be conveniently rewritten as an inhomogeneous integral equation as follows:

$$G_{fs}(\vec{r}, \vec{r}'; \omega) = G_{3D}(\vec{r}, \vec{r}'; \omega) + \frac{\omega^2}{c^2} \int d^3\vec{r}'' \int d^3\vec{r}''' G_{3D}(\vec{r}, \vec{r}''; \omega) \alpha_{fs}^{2D}(\vec{r}'', \vec{r}'''; \omega) G_{fs}(\vec{r}''', \vec{r}'; \omega). \quad (2.1.7)$$

Introducing Eq. (2.1.2) in Eq. (2.1.7) and Fourier transforming the resulting equation in the lateral plane of translational invariance ($\vec{r}_{\parallel} - \vec{r}'_{\parallel} \rightarrow \vec{k}_{\parallel}$), we obtain

$$G_{fs}(\vec{k}_{\parallel}; z, z'; \omega) = G_{3D}(\vec{k}_{\parallel}; z, z'; \omega) + \frac{\omega^2 d}{c^2} G_{3D}(\vec{k}_{\parallel}; z, 0; \omega) \alpha_{fs}^{(2D)}(\vec{k}_{\parallel}; \omega) G_{fs}(\vec{k}_{\parallel}; 0, z'; \omega). \quad (2.1.8)$$

Solving for $G_{fs}(\vec{k}_{\parallel}; 0, z'; \omega)$ algebraically, we obtain

$$G_{fs}(\vec{k}_{\parallel}; z, z'; \omega) = G_{3D}(\vec{k}_{\parallel}; z, z'; \omega) + \frac{\omega^2 d}{c^2} \frac{G_{3D}(\vec{k}_{\parallel}; z, 0; \omega) \alpha_{fs}^{(2D)}(\vec{k}_{\parallel}; \omega) G_{3D}(\vec{k}_{\parallel}; 0, z'; \omega)}{1 - \frac{\omega^2 d}{c^2} \alpha_{fs}^{(2D)}(\vec{k}_{\parallel}; \omega) G_{3D}(\vec{k}_{\parallel}; 0, 0; \omega)}, \quad (2.1.9)$$

and using Eq. (2.1.6), this leads to the full sheet Green's function as

$$G_{fs}(\vec{k}_{\parallel}; z, z'; \omega) = -\frac{e^{ik_{\perp}|z-z'|}}{2ik_{\perp}} + \frac{\gamma e^{ik_{\perp}(|z|+|z'|)}}{2ik_{\perp}(2ik_{\perp} + \gamma)}, \quad (2.1.10)$$

where

$$\gamma = \omega^2 d\alpha_{fs}^{(2D)}(\vec{k}_{\parallel}; \omega)/c^2. \quad (2.1.11)$$

Our analysis (below) of the Green's function in the presence of an aperture will be seen to devolve upon the evaluation of $G_{fs}(\vec{r}, \vec{r}''; z, z''; \omega)$ at the aperture position $\vec{r}'' = 0, z'' = 0$ in position representation as given by

$$G_{fs}(\vec{r}_{\parallel}, 0; z, 0; \omega) = \frac{1}{(2\pi)^2} \int d^2\vec{k}_{\parallel} e^{i\vec{k}_{\parallel} \cdot \vec{r}_{\parallel}} G_{fs}(\vec{k}_{\parallel}; z, 0; \omega) \quad (2.1.12)$$

where

$$G_{fs}(\vec{k}_{\parallel}; z, 0; \omega) = -\frac{e^{ik_{\perp}|z|}}{2ik_{\perp} + \gamma}, \quad (2.1.13)$$

so that

$$G_{fs}(\vec{r}_{\parallel}, 0; z, 0; \omega) = -\frac{1}{4i\pi} \int_0^{\infty} dk_{\parallel} \frac{k_{\parallel} J_0(k_{\parallel} r_{\parallel}) e^{ik_{\perp}|z|}}{k_{\perp} + \frac{\gamma}{2i}}. \quad (2.1.14)$$

Noting Eq. (2.1.11) and employing the 2D polarizability of the layer as [6]

$$\alpha_{fs}^{(2D)}(\vec{k}_{\parallel}; \omega) = \left(\frac{2\pi i e^2 n_{2D}}{m^* \omega^2} \right) \sqrt{q_{\omega}^2 - k_{\parallel}^2} \quad (2.1.15)$$

(n_{2D} is the 2D equilibrium density on the sheet, m^* is the effective mass and $\mu = \frac{\pi e^2 d n_{2D}}{m^* c^2}$), we have

$$G_{fs}(\vec{r}_{\parallel}, 0; z, 0; \omega) = -\frac{1}{4i\pi[1 + \mu]} \int_0^{\infty} \frac{dk_{\parallel} k_{\parallel} J_0(k_{\parallel} r_{\parallel}) e^{i|z|\sqrt{q_{\omega}^2 - k_{\parallel}^2}}}{\sqrt{q_{\omega}^2 - k_{\parallel}^2}}. \quad (2.1.16)$$

The k_{\parallel} - integral of Eq. (2.1.16) is readily evaluated as[7]

$$G_{fs}(\vec{r}_{\parallel}, 0; z, 0; \omega) = \frac{1}{4\pi[1 + \mu]} \frac{e^{iq_{\omega}\sqrt{r_{\parallel}^2 + |z|^2}}}{\sqrt{r_{\parallel}^2 + |z|^2}}. \quad (2.1.17)$$

3. GREEN'S FUNCTION SOLUTION FOR A PERFORATED 2D PLASMONIC LAYER WITH A NANO-HOLE EMBEDDED IN A 3D BULK HOST MEDIUM

3.1. Integral Equation: Scalar Helmholtz Green's Function for a Perforated Plasmonic Layer

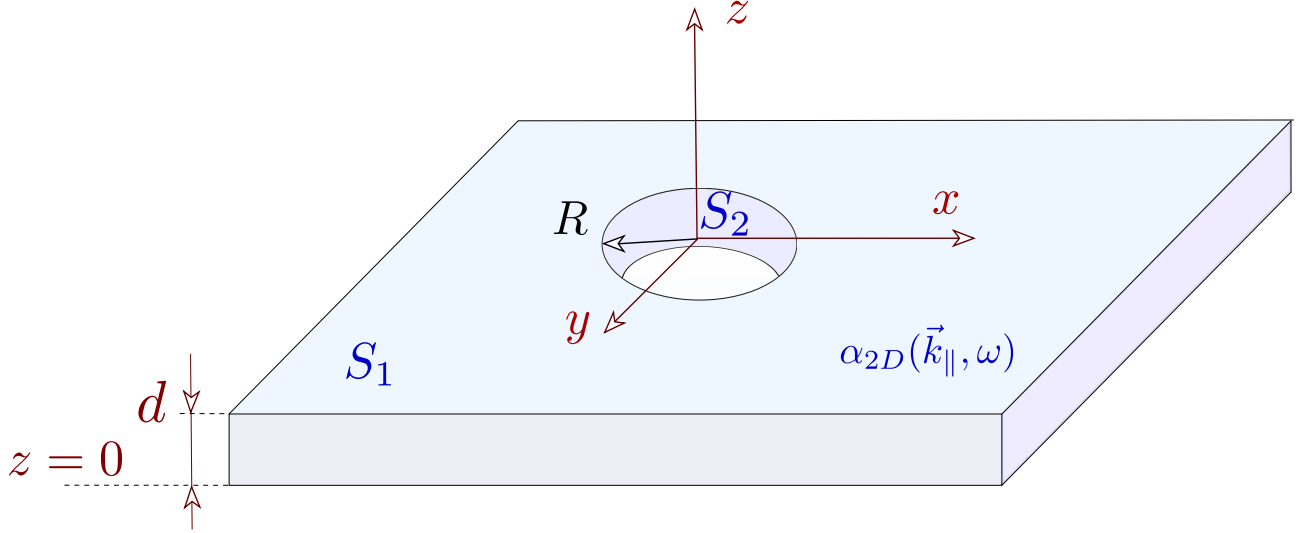


FIG. 3.1.1: (Color online) Schematic representation of a perforated 2D plasmonic layer (thickness d , embedded at $z = 0$ in a three dimensional bulk medium) with a nano-hole of radius R at the origin of the $(x - y)$ -plane.

We consider a 2D plasmonic layer S_1 which is perforated by a nano-scale aperture S_2 of radius R , as depicted in Fig.3.1.1, lying in the $(x - y)$ -plane. The presence of the nano-hole in the layer is represented by subtracting the part of the polarizability associated with the hole from the polarizability of the full layer, (Fig.3.1.1)[1,2,3,4]

$$\alpha^{(2D)}(\vec{r}, \vec{r}'; \omega) = \alpha_{fs}^{(2D)}(\vec{r}, \vec{r}'; \omega) - \alpha_h^{(2D)}(\vec{r}, \vec{r}'; \omega) \quad (3.1.1)$$

where $\alpha_h^{(2D)}(\vec{r}, \vec{r}'; \omega)$ is the part of the layer polarizability removed by the nano-hole. The resulting Green's function for the perforated plasmonic layer with the hole satisfies the integral equation given by

$$G(\vec{r}, \vec{r}'; \omega) = G_{fs}(\vec{r}, \vec{r}'; \omega) - \frac{\omega^2}{c^2} \int d^3\vec{r}'' \int d^3\vec{r}''' G_{fs}(\vec{r}, \vec{r}''; \omega) \times \alpha_h^{2D}(\vec{r}'', \vec{r}'''; \omega) G(\vec{r}''', \vec{r}'; \omega). \quad (3.1.2)$$

Here, the polarizability of the nano-hole is defined as [8,9]

$$\alpha_h^{(2D)}(\vec{r}, \vec{r}'; \omega) = \alpha_{fs}^{(2D)}(x, y, x', y'; \omega) \eta_+(R - |x|) \eta_+(R - |y|) \eta_+(R - |x'|) \eta_+(R - |y'|) d\delta(z) \delta(z'), \quad (3.1.3)$$

where $\eta_+(R - |x|)$ is the Heaviside unit step function representing a cut-off imposed to confine the integration range on the 2D sheet to the nano-hole dimensions; and the Dirac delta function $\delta(z)$ is needed to localize the polarizability onto the plane of the 2D plasmonic layer. A simple approximation of Eq. (3.1.3) for very small radius leads to (A represents the area of the aperture)

$$\alpha_h^{(2D)}(\vec{r}, \vec{r}'; \omega) \approx A^2 \alpha_{fs}^{(2D)}(\vec{r}_{\parallel}, \vec{r}'_{\parallel}; \omega) \delta^{2D}(\vec{r}_{\parallel}) \delta^{2D}(\vec{r}'_{\parallel}) d\delta(z) \delta(z'), \quad (3.1.4)$$

and employing it in Eq. (3.1.2) to execute all positional integrations, we obtain

$$G(\vec{r}_{\parallel}, \vec{r}'_{\parallel}; z, z'; \omega) \approx G_{fs}(\vec{r}_{\parallel}, \vec{r}'_{\parallel}; z, z'; \omega) - \beta G_{fs}(\vec{r}_{\parallel}, 0; z, 0; \omega) G(0, \vec{r}'_{\parallel}; 0, z'; \omega), \quad (3.1.5)$$

where $\beta = \gamma A^2$ with $\gamma = \frac{\omega^2 d}{c^2} \alpha_{fs}^{2D}([\vec{r}_{\parallel} = 0] - [\vec{r}'_{\parallel} = 0]; \omega)$. To solve Eq. (3.1.5), we set $\vec{r}_{\parallel} = 0$ and $z = 0$, and determine $G(0, \vec{r}'_{\parallel}; 0, z'; \omega)$ as

$$G(0, \vec{r}'_{\parallel}; 0, z'; \omega) = \frac{G_{fs}(0, \vec{r}'_{\parallel}; 0, z'; \omega)}{1 + \beta G_{fs}(0, 0; 0, 0; \omega)}. \quad (3.1.6)$$

Substituting Eq. (3.1.6) into Eq. (3.1.5) yields the algebraic closed form analytic solution:

$$G(\vec{r}_{\parallel}, \vec{r}'_{\parallel}; z, z'; \omega) \approx G_{fs}(\vec{r}_{\parallel}, \vec{r}'_{\parallel}; z, z'; \omega) - \frac{\beta G_{fs}(\vec{r}_{\parallel}, 0; z, 0; \omega) G_{fs}(0, \vec{r}'_{\parallel}; 0, z'; \omega)}{1 + \beta G_{fs}([\vec{r}_{\parallel} = 0] - [\vec{r}'_{\parallel} = 0]; z = 0, z' = 0; \omega)}. \quad (3.1.7)$$

Noting that a transmitted scalar wave is controlled by $G(\vec{r}_{\parallel}, 0; z, 0; \omega)$, we have analyzed this quantity setting $\vec{r}'_{\parallel} = 0$ and $z' = 0$ in Eq. (3.1.7), leading to

$$G(\vec{r}_{\parallel}, 0; z, 0; \omega) \approx \frac{G_{fs}(\vec{r}_{\parallel}, 0; z, 0; \omega)}{1 + \beta G_{fs}([\vec{r}_{\parallel} = 0] - [\vec{r}'_{\parallel} = 0]; z = 0, z' = 0; \omega)}. \quad (3.1.8)$$

Eq. (3.1.8) is an approximate analytical Green's function solution to Eq. (3.1.2), in which $G_{fs}([\vec{r}_{\parallel} = 0] - [\vec{r}'_{\parallel} = 0]; z = 0, z' = 0; \omega)$ is found to involve a divergent integral when all its arguments vanish. This divergence may be seen in $\alpha_{fs}^{(2D)}$ and G_{fs} setting $\vec{r}_{\parallel} = 0$, $\vec{r}'_{\parallel} = 0$, $z = 0$ and $z' = 0$ as follows:

$$\alpha_{fs}^{(2D)}(0, 0; \omega) = \frac{1}{2\pi} \left(\frac{2\pi i e^2 n_{2D}}{m^* \omega^2} \right) \int_0^\infty dk_{\parallel} k_{\parallel} \sqrt{q_\omega^2 - k_{\parallel}^2}, \quad (3.1.9)$$

and Eq. (2.1.16) is given by

$$G_{fs}(0, 0; 0, 0; \omega) = \frac{i}{4\pi[1 + \mu]} \int_0^\infty \frac{dk_{\parallel} k_{\parallel}}{\sqrt{q_\omega^2 - k_{\parallel}^2}}. \quad (3.1.10)$$

The divergence of $\alpha_{fs}^{(2D)}$ and G_{fs} is an artifact of limiting the radius of the aperture to be vanishingly small (zero) in the kernel of the integral equation, Eq. (3.1.2) - Eq. (3.1.4). A more realistic consideration involves a cut off at a small but finite radius R , alternatively an upper limit on the wavenumber integration, $k_{\parallel} \sim \frac{1}{R}$, yielding the convergent integrals

$$\alpha_{fs}^{(2D)}(0, 0; \omega) = \frac{q_\omega^3}{2\pi} \left(\frac{2\pi i e^2 n_{2D}}{m^* \omega^2} \right) \left\{ \int_0^1 dy y \sqrt{1 - y^2} + i \int_1^{\frac{1}{q_\omega R}} dy y \sqrt{y^2 - 1} \right\} \quad (3.1.11)$$

and

$$G_{fs}([\vec{r}_{\parallel} = 0] - [\vec{r}'_{\parallel} = 0]; z = 0, z' = 0; \omega) \approx \frac{i q_\omega}{4\pi[1 + \mu]} \left\{ \int_0^1 dy \frac{y}{\sqrt{1 - y^2}} - i \int_1^{\frac{1}{q_\omega R}} dy \frac{y}{\sqrt{y^2 - 1}} \right\}, \quad (3.1.12)$$

where we have introduced the dimensionless notation $y = k_{\parallel}/q_\omega$, so that

$$k_{\perp} = \begin{cases} q_\omega \sqrt{1 - y^2} & \text{for } 0 \leq y < 1; \\ i q_\omega \sqrt{y^2 - 1} & \text{for } y > 1. \end{cases} \quad (3.1.13)$$

and the following results are obtained

$$\alpha_{fs}^{(2D)}([\vec{r}_{\parallel} = 0], [\vec{r}'_{\parallel} = 0]; \omega) \approx \frac{1}{6\pi R^3} \left(\frac{2\pi i e^2 n_{2D}}{m^* \omega^2} \right) \left[(q_\omega R)^3 + i [1 - (q_\omega R)^2]^{3/2} \right] \quad (3.1.14)$$

and

$$G_{fs}([\vec{r}_{\parallel} = 0] - [\vec{r}'_{\parallel} = 0]; z = 0, z' = 0; \omega) \approx \frac{1}{4\pi(1 + \mu)R} \left[i q_\omega R + \sqrt{1 - (q_\omega R)^2} \right], \quad (3.1.15)$$

for $q_\omega R < 1$. Furthermore, substituting Eq. (3.1.14) into the expression for γ , we have

$$\gamma = \frac{\mu}{3\pi R^3} \left[i (q_\omega R)^3 - [1 - (q_\omega R)^2]^{3/2} \right] \quad (3.1.16)$$

with $\mu = \pi e^2 d n_{2D} / (m^* c^2)$.

4. NUMERICAL RESULTS

Our numerical results for the real and imaginary parts of the Green's function in Eq. (3.1.8), $\text{Re}[G(\vec{r}_{\parallel}, 0; z, 0; \omega)]$ and $\text{Im}[G(\vec{r}_{\parallel}, 0; z, 0; \omega)]$, respectively, for frequency $f = 300$ THz

are presented in Figs: 4.1, 4.2 and 4.3 as functions of x and y for several values of distance z away from the layer screen: We chose $z = 50 R$ (near-field), $z = 300 R$ (middle-field) and $z = 1000 R$ (far-field). These figures reveal the structure of the Green's function for the perforated layer in terms of near-field ($z = 50 R$), middle-field ($z = 300 R$) and far-field ($z = 1000 R$) radiation zones for $R = 5 \text{ nm}$.

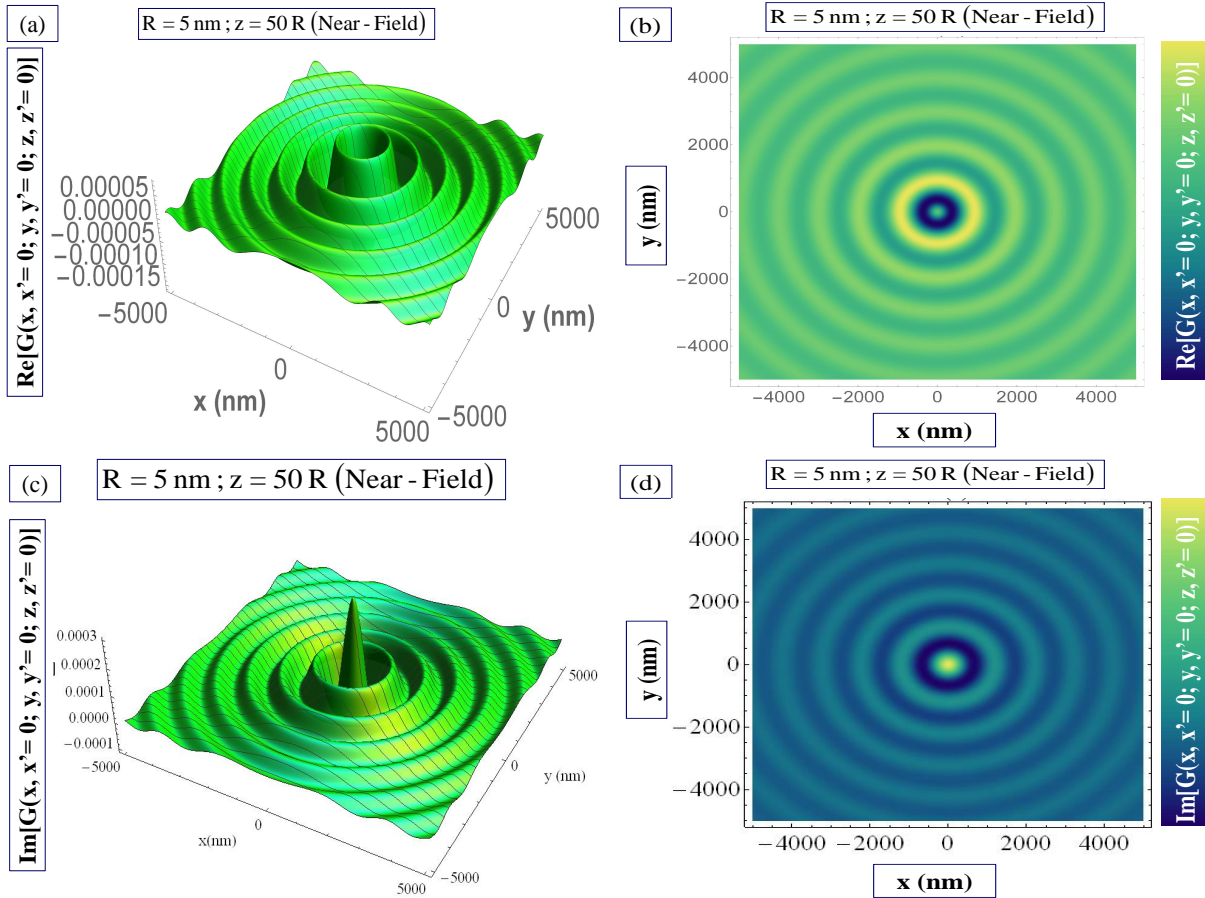


FIG. 4.1: (Color online) Figures (a) and (b) exhibit $\text{Re}[G(\vec{r}_{\parallel}, 0; z, 0; \omega)]$ and (c) and (d) present $\text{Im}[G(\vec{r}_{\parallel}, 0; z, 0; \omega)]$ (in 3D (a, c) and density (b, d) plots) for a perforated 2D plasmonic layer of GaAs in the presence of a nano-hole of radius $R = 5 \text{ nm}$ at $z = 50 R$ (Near-Field) for $\epsilon_b = 1$, $n_{2D} = 4 \times 10^{15} \text{ cm}^{-2}$, $d = 10 \text{ nm}$ and $m^* = 0.065 m_0$ where m_0 is the free-electron mass.

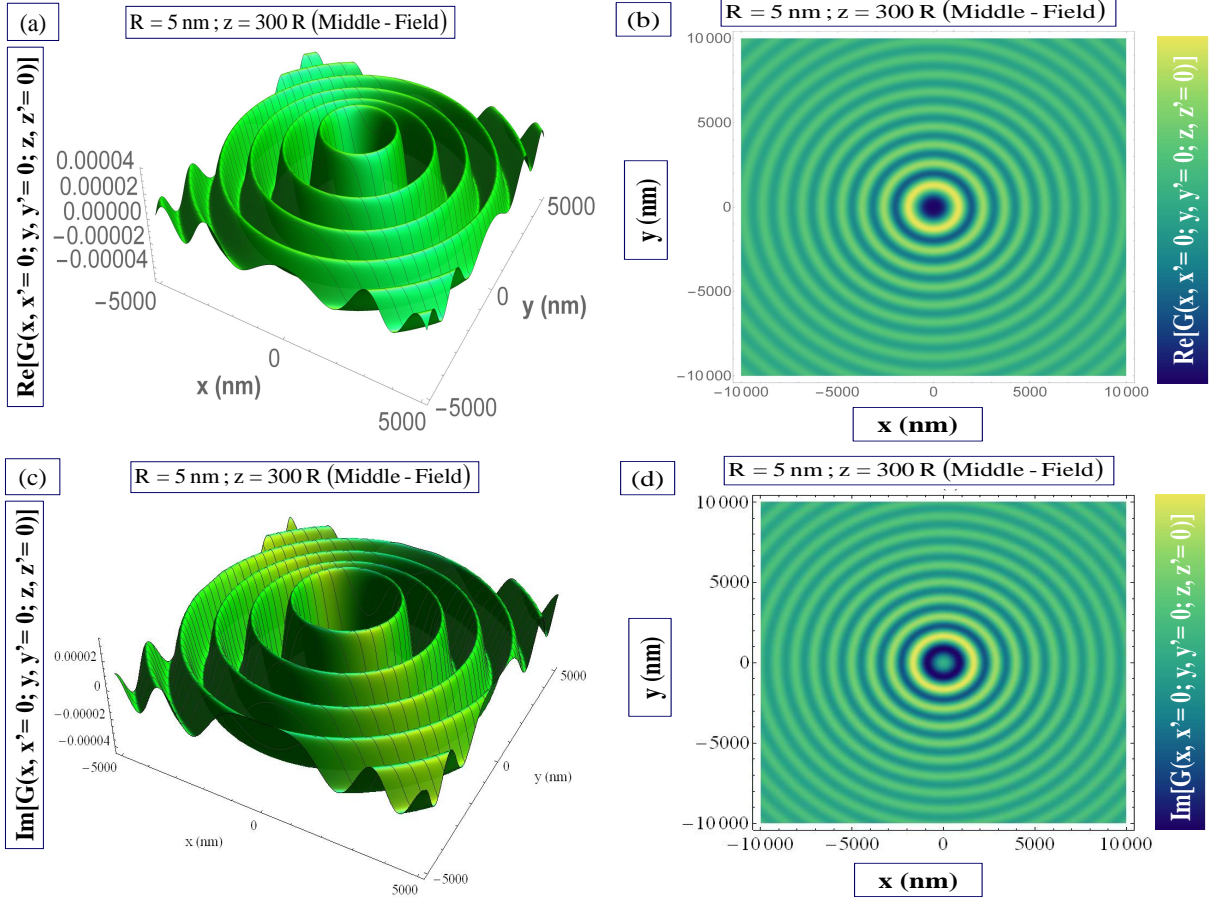


FIG. 4.2: (Color online) Figures (a) and (b) exhibit $\text{Re}[G(\vec{r}_{\parallel}, 0; z, 0; \omega)]$ and (c) and (d) present $\text{Im}[G(\vec{r}_{\parallel}, 0; z, 0; \omega)]$ (in 3D (a, c) and density (b, d) plots) for a perforated 2D plasmonic layer of GaAs in the presence of a nano-hole of radius $R = 5 \text{ nm}$ at $z = 300 R$ (Middle-Field) for $\epsilon_b = 1$, $n_{2D} = 4 \times 10^{15} \text{ cm}^{-2}$, $d = 10 \text{ nm}$ and $m^* = 0.065m_0$ where m_0 is the free-electron mass.

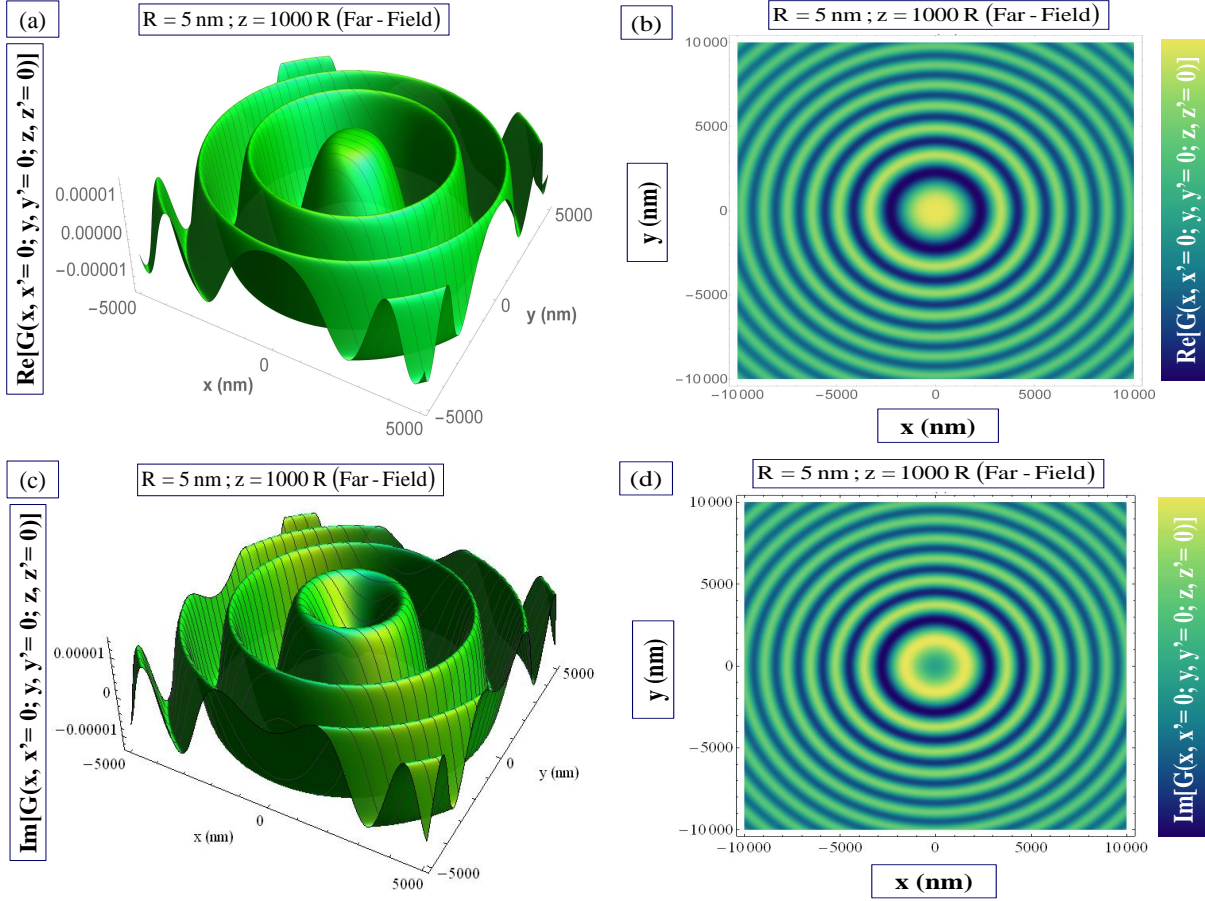


FIG. 4.3: (Color online) Figures (a) and (b) exhibit $\text{Re}[G(\vec{r}_{\parallel}, 0; z, 0; \omega)]$ and (c) and (d) present $\text{Im}[G(\vec{r}_{\parallel}, 0; z, 0; \omega)]$ (in 3D (a, c) and density (b, d) plots) for a perforated 2D plasmonic layer of GaAs in the presence of a nano-hole of radius $R = 5 \text{ nm}$ at $z = 1000 R$ (Far-Field) for $\epsilon_b = 1$, $n_{2D} = 4 \times 10^{15} \text{ cm}^{-2}$, $d = 10 \text{ nm}$ and $m^* = 0.065m_0$ where m_0 is the free-electron mass.

Further detail concerning $\text{Re}[G(\vec{r}_{\parallel}, 0; z, 0; \omega)]$ and $\text{Im}[G(\vec{r}_{\parallel}, 0; z, 0; \omega)]$ is provided in the figures below for the three z -radiation zones described by $z = 50 R$ (near-field), $z = 300 R$ (middle-field) and $z = 1000 R$ (far-field):

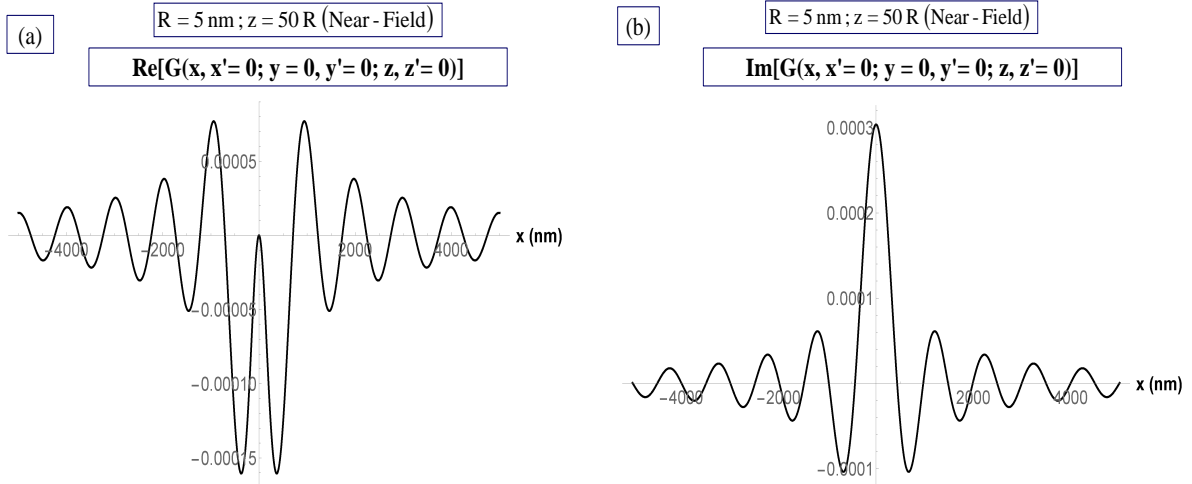


FIG. 4.4: (a) exhibits $\text{Re}[G(x, x'=0; y=0, y'=0; z=50R, z'=0; \omega)]$ and (b) presents $\text{Im}[G(x, x'=0; y=0, y'=0; z=50R, z'=0; \omega)]$ as a function of x for a perforated 2D plasmonic layer of GaAs in the presence of a nano-hole of radius $R = 5$ nm at $z = 50R$ (Near-Field) for $\epsilon_b = 1$, $n_{2D} = 4 \times 10^{15} \text{ cm}^{-2}$, $d = 10$ nm and $m^* = 0.065m_0$ where m_0 is the free-electron mass.

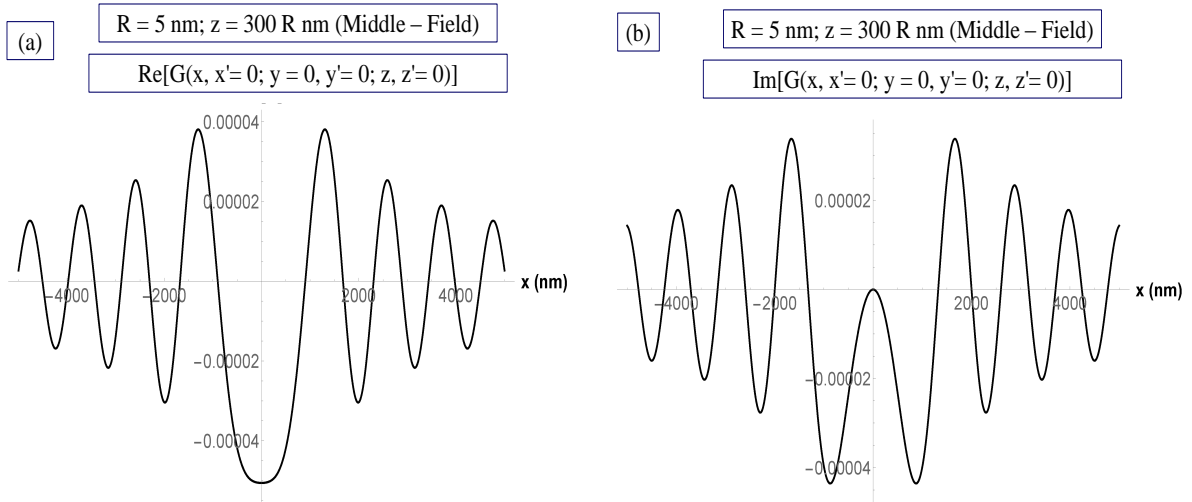


FIG. 4.5: (a) exhibits $\text{Re}[G(x, x'=0; y=0, y'=0; z=300R, z'=0; \omega)]$ and (b) presents $\text{Im}[G(x, x'=0; y=0, y'=0; z=300R, z'=0; \omega)]$ as a function of x for a perforated 2D plasmonic layer of GaAs in the presence of a nano-hole of radius $R = 5$ nm at $z = 300R$ (Middle-Field) for $\epsilon_b = 1$, $n_{2D} = 4 \times 10^{15} \text{ cm}^{-2}$, $d = 10$ nm and $m^* = 0.065m_0$ where m_0 is the free-electron mass.

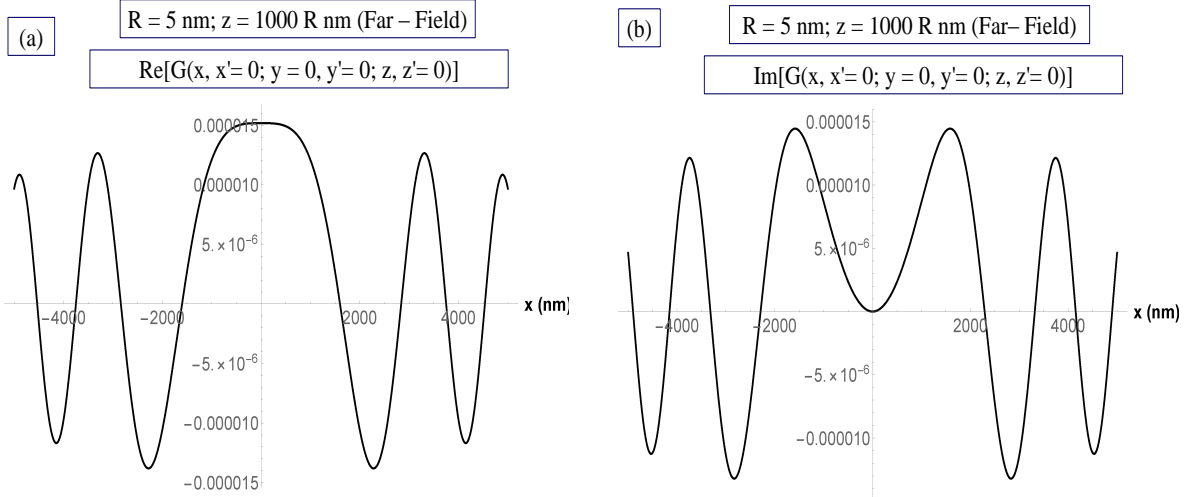


FIG. 4.6: (a) exhibits $\text{Re}[G(x, x' = 0; y = 0, y' = 0; z = 1000 R, z' = 0; \omega)]$ and (b) presents $\text{Im}[G(x, x' = 0; y = 0, y' = 0; z = 1000 R, z' = 0; \omega)]$ as a function of x for a perforated 2D plasmonic layer of GaAs in the presence of a nano-hole of radius $R = 5 \text{ nm}$ at $z = 1000 R$ (Far-Field) for $\epsilon_b = 1$, $n_{2D} = 4 \times 10^{15} \text{ cm}^{-2}$, $d = 10 \text{ nm}$ and $m^* = 0.065 m_0$ where m_0 is the free-electron mass.

5. CONCLUDING REMARKS

In this paper we have carried out a thorough numerical analysis of the closed-form expression for the scalar Green's function of a perforated, thin 2D plasmonic layer embedded in a 3D host medium in the presence of a nano-hole.

Inspection of the resulting Green's function figures shows that for large $r_{\parallel} \mapsto x > 2500 \text{ nm}$ the spatial dependence of the Green's function becomes oscillatory as a function of $r_{\parallel}(x)$ with peaks uniformly spaced. In this regard, it should be noted that our designation of near, middle and far radiation zones is defined in terms of z -values ($50R, 300R, 1000R$) *alone*, to the exclusion of r_{\parallel} : In consequence of this exclusion, the figures actually carry useful information for $r_{\parallel}(x)$ in *all* radiation zones as conventionally defined in terms of the incident wavelength $\lambda \sim 2\pi/q\omega$. Furthermore, this approach to oscillatory behavior as a function of r_{\parallel} with uniformly spaced peaks is accompanied by a geometric $1/r_{\parallel}$ - diminution of the amplitude of the Green's function. On the other hand, our far zone figures also show that when $z > r_{\parallel} = x$ the Green's function flattens as a function of $r_{\parallel} = x$ into a region of

constancy, which is evident in Fig.4.6.

6. APPENDIX

We consider the evaluation of the following integral [7]

$$I(a, b, c) = \int_0^\infty dx \frac{x J_0(ax) e^{ic\sqrt{b^2-x^2}}}{\sqrt{b^2-x^2}} = \frac{e^{ib\sqrt{a^2+c^2}}}{i\sqrt{a^2+c^2}}. \quad (6.1)$$

Setting $c = 0$ in Eq. (6.1) yields

$$I(a, b, 0) = \int_0^\infty dx \frac{x J_0(ax)}{\sqrt{b^2-x^2}} = \frac{e^{iba}}{ia}. \quad (6.2)$$

Differentiating $\partial^2/\partial c^2$ of Eq. (6.1), we obtain

$$\begin{aligned} \frac{\partial^2 I(a, b, c)}{\partial c^2} &= \frac{\partial^2}{\partial c^2} \left\{ \int_0^\infty dx \frac{x J_0(ax) e^{ic\sqrt{b^2-x^2}}}{\sqrt{b^2-x^2}} \right\} \\ &= \frac{\partial^2}{\partial c^2} \left\{ \frac{e^{ib\sqrt{a^2+c^2}}}{i\sqrt{a^2+c^2}} \right\}. \end{aligned} \quad (6.3)$$

Again setting $c = 0$ in Eq. (6.3) after taking the second derivative, the following result is obtained

$$\int_0^\infty dx x \sqrt{(a^2-x^2)} J_0(x) = -(a+i)e^{ia}. \quad (6.4)$$

The first derivative of Eq. (6.1) yields

$$\begin{aligned} \frac{\partial I(a, b, c)}{\partial c} &= \frac{\partial}{\partial c} \left\{ \int_0^\infty dx \frac{x J_0(ax) e^{ic\sqrt{b^2-x^2}}}{\sqrt{b^2-x^2}} \right\} = \frac{\partial}{\partial c} \left\{ \frac{e^{ib\sqrt{a^2+c^2}}}{i\sqrt{a^2+c^2}} \right\} \\ &= \int_0^\infty dx x J_0(ax) e^{ic\sqrt{b^2-x^2}} = -\frac{\partial}{\partial c} \left\{ \frac{e^{ib\sqrt{a^2+c^2}}}{\sqrt{a^2+c^2}} \right\} \\ &= -\frac{ic(i+\sqrt{a^2+c^2})e^{i\sqrt{a^2+c^2}}}{(a^2+c^2)^{3/2}}. \end{aligned} \quad (6.5)$$

Acknowledgments

We gratefully acknowledge support from the NSF-AGEP program for the work reported in this paper. Thanks are extended to Professors M. L. Glasser and Dr. Erik Lenzing for numerous helpful discussions as well as Liuba Zhemchuzhna and Dr. Andrii Iurov for helpful comments.

-
- ¹ Désiré Miessein, " Ph.D Thesis: Scalar and Electromagnetic Waves Transmission Through a Sub-wavelength Nano-hole in a 2D Plasmonic Semiconductor Layer " Stevens Institute of Technology, Hoboken, New Jersey (2013).
 - ² N. J. M. Horing and D. Miessein, " Wave Propagation and Diffraction Through a Subwavelength Nano-Hole in a 2D Plasmonic Screen", in book chapter : " Low-Dimensional and Nanostructured Materials and Devices ", Hilmi Ünlü, Norman J. M. Horing, Jaroslaw Dabowski, Springer International Publishing Switzerland (2016).
 - ³ N. J. M. Horing, D. Miessein and G. Gumbs, " Electromagnetic Wave Transmission Through a Subwavelength Nano-hole in a Two-Dimensional Plasmonic Layer ", J. Opt. Soc. Amer. A **32**, 1184-1198 (2015).
 - ⁴ D. Miessein, N. J. M. Horing, H. Lenzing and G. Gumbs, " Incident-Angle Dependence of Electromagnetic Transmission through a Plasmonic Screen with Nano-Aperture ", Adv. Nano Bio. MD: (2017): 1(1):54-70 ISSN: 2559-1118.
 - ⁵ Morse and Feshbach," Methods in Theoretical Physics,vol.2 ", McGraw-Hill, (1953), p.234.
 - ⁶ Mark Orman " Ph.D Thesis: Electromagnetic Response of a Quantized Magnetoplasma in 2 and 3 Dimensions " (1974).
 - ⁷ Bateman, " Higher Transcendental Functions, Vol.2 ", McGraw-Hill, (1953), p.95, Eq.52
 - ⁸ Weng Cho Chew, " Waves and Fields In Inhomogeneous Media " IEEE, Inc, (1995), p.385.
 - ⁹ Weng Cho Chew, " Waves and Fields In Inhomogeneous Media" IEEE, Inc, (1995), p.377, Eq. (7.1.14).